Chloride Contributions in Flux-Assisted GTA Welding of Magnesium Alloys

Experiments demonstrated chlorides increased arc voltage, arc temperature, and weld penetration, with cadmium chloride being the most effective

BY M. MARYA AND G. R. EDWARDS

ABSTRACT. For transition-metal alloys, chemical fluxes predeposited on the path of gas tungsten electric arcs can significantly increase weld penetration. Several mechanisms for this beneficial contribution of fluxes, including electrical charge redistribution (possibly constriction) and surface-energy-driven flow (Marangoni effect), have been postulated. Using argon shielding and chloride fluxes, magnesium alloy welding experiments revealed increases in weld penetration as much as one hundred percent were not unusual. Among all selected chlorides (LiCl, $CaCl_2$, $CdCl_2$, $PbCl_2$ and $CeCl_3$), cadmium chloride was the most effective. Real-time monitoring demonstrated that all chlorides increased both the arc voltage and the arc temperature. Furthermore, video recordings showed the electric arc was broader with chlorides, particularly in the direction of welding. Increases in heat input, accompanied by a redistribution of the heat flux, are therefore suggested as the main contribution to the augmented weld penetration with chlorides.

Introduction

A number of studies regarding flux-assisted gas tungsten arc welding (FA-GTAW) have been published. In the mid-1960s, research (Refs. 1, 2) showed weld penetration could be augmented as much as three times when the base materials were coated with fluxes. Such fluxes remain interesting today because they allow full-penetration welding at greater rates while still employing the inexpensive and clean gas tungsten arc as the heat source. To date, however, fluxes have been developed only for joining titanium alloys (Refs. 2–6) and steels (Refs. 7, 8) and their compositions are not published.

Several mechanisms for the augmented penetration observed in FA-GTA welding have been given (Refs. 5–10). The relative importance of each mechanism is a function of the chemical composition of the flux and the base metal, as well as the process parameters. A spatial redistribution of the current density is most probable. A redistributed current would affect the heat flux from the arc, the induced Lorenz electromagnetic force, the pressure on the weld pool, and thus its heat and mass transports. Although not entirely resolved, the mechanism of arc constriction that raises the current density and creates welds with greater depth-to-width ratios has often been invoked (Refs. 5, 8, 9). Because the flux also chemically interacts with the molten material, a surface-energy contribution that originates a Marangoni flow has also been proposed (Refs. 8, 10).

The influence of surface-active species on weld morphology has been well documented in transition-metal alloys (Refs. 11–15) since the work of Heiple and Roper (Refs. 11, 12, 15). These investigators discovered that sulfur often offsets normal weld fluid flow. Particularly after droplet levitation experiments by Mills and Keene (Ref. 13), sulfur segregation to a free surface and the corresponding effect on surface tension, γ, became understood. It was found sulfur could increase surface tension of liquid iron under increasing temperature conditions, thus making the temperature gradient, $d\gamma/dT$, positive. Because of the temperature profile over the weld pool, the surface tension normally pulls the liquid toward the solid phase, where temperature and surface tension are respectively smaller and greater. With trace amounts of sulfur in ferrous alloys (Refs. 11, 12, 15), however, a reversal of the fluid flow occurs when the surface tension becomes greater in the hottest regions. The fluid flow, then toward the weld centerline, diminishes the heat extraction sidewise and leaves narrower and deeper welds.

KEY WORDS

Magnesium
GTA Welding
Chloride Fluxes
Weld Morphology
Process Monitoring
First Ionization Potential

For light metals, elements like sulfur in steels that create this inward Marangoni flow have not been reported, making unlikely the existence of a surface-energy-driven flow due to a sign change of $d\gamma/dT$. However, with the flux ingredients unevenly distributed over the pool, composition may assist surface tension to participate in the weld pool circulation. As for steels and titanium alloys, a surface-tension component assisted by a redistribution of both heat and pressure from the arc may thus be at the origin of deeper and narrower welds in magnesium alloys.

From all the potential flux ingredients, metal chlorides were selected for this study. Chlorides are ionic compounds and are semiconductive. Their lower electrical conductivity (Ref. 16) relative to metals indicates the electric arc may be harder to strike if they are utilized as flux, and this may result in an arc constriction. The fact that metal chlorides serve for the casting of magnesium alloys suggests detrimental effects during solidification are negligible. Not only are chlorides ingredients for casting (Ref. 17), but they are also applied as fluxes for the submerged arc welding of steels and titanium alloys (Refs. 18, 19) where they primarily protect the molten metal. Chlorides also serve in "reaction" soldering fluxes (Ref. 20), where, by infiltrating and disrupting the thin and refractory oxide layer on light metals, they im-

M. MARYA and G. R. EDWARDS are with the Center for Welding, Joining, and Coatings Research, The G. S. Ansell Department of Metallurgical and Materials Engineering, Colorado School of Mines, Golden, Colo.

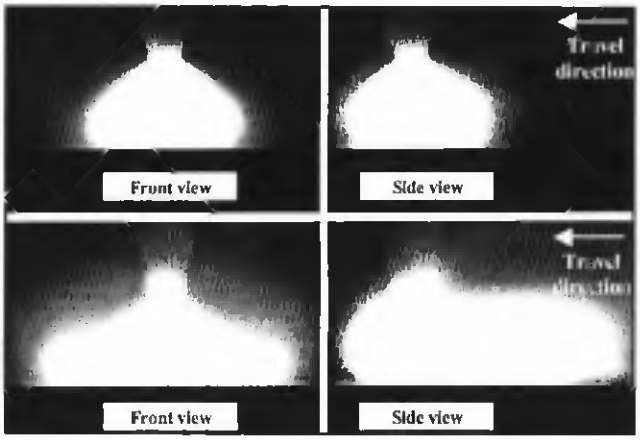

Fig. 1 — Images of an 80-A arc produced without (top) and with cadmium chloride (bottom).

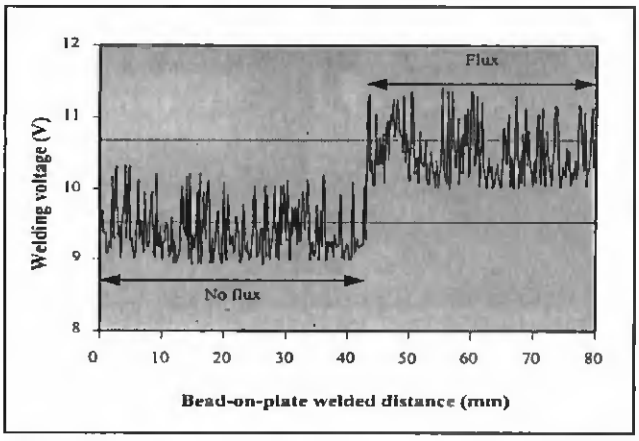

Fig. 2 — Voltage-distance diagram at 60 A showing the effect on voltage of the cadmium chloride flux.

prove the wetting characteristics of the solder.

In arc welding of light metals, surface oxide is problematic. Usual techniques employ alternating currents to provide cathodic cleaning (Ref. 21). With these currents, time-averaged heat input, and thus melting efficiency and weld penetration, are lower than with a direct current thermo emitted from a cathode. Therefore, with a direct current, a tungsten-matrix cathode and an adequate chloride flux, thicker sections may be fused together by the GTAW process. In this article, the criteria for identifying the best chloride ingredients are discussed. Relevant are physics and alloying theory are discussed and applied to bead-on-plate FA-GTA welding experiments.

Characteristics of GTA Arcs and Fluxes

Practically, a suitable flux must change the weld dimensions with uniformity and repeatability. If flux thickness varies, irregular weld beads and deteriorated properties may result. Spreading and wetting are thus both required, and these properties can be realized only with a highly fluid flux. Wetting implies the flux adheres to the base metal enough to resist the impact of the shielding gas. Investigations (Refs. 8, 9) showed fluxes are typically made after adding powder ingredients to a solvent of acetone, ethanol, or water. Once applied by brush or spray, welding proceeds usually after a thin layer of flux has become dry. The resulting welds must exhibit smooth surfaces for mechanical properties and corrosion resistance, thus making indispensable steady arcs.

Such practicalities can be resolved if the roles of fluxes are assessed both theoretically and experimentally. The interactions of fluxes, particularly chlorides, with the electric arc and the base metal are discussed later.

Potential Flux-Arc Interactions

The welding arc can be defined as a sustained discharged plasma with a highly nonuniform electric potential. Although a precise description of the chemical and electronic events within the arc is beyond the scope of this investigation, a description of the arc can be attempted using basic principles of plasma physics and experimental evidence from past investigations (Refs. 22, 23).

The arc is frequently separated into three regions (Refs. 22, 23): cathode, anode, and arc column. Gaseous particles within these regions originate from the shielding gas, the ambient air, and the vaporization of the flux, the base metal, and, to a lesser extent, the tungsten electrode. The arc is formed by the dissipation of the supplied electrical energy. The generated thermal energy measures the kinetic energy of particles colliding elastically as well as nonelastically. The nonelastic collisions create charged particles from initially neutral particles, thus making this initially nonconductive neutral gas mixture an electrical conductor. Initially, neutral atoms and molecules of this gas must be ionized, requiring dissociation of heavy molecules into lighter molecules, neutral atoms, positive ions (cations), negative ions (anions), and free electrons. An ion can be either an atom or a molecule, from which one or several electrons have been added or removed. Electrons are generated by two mechanisms: thermionic emission from the electrodes, as expressed by the Richardson-Dushman equation (Ref. 23) and ionization of initially neutral particles (first ionization) by collisions and self-induced heating. Their density and distribution vary within the arc regions. Due to coulombic interactions, cations and electrons are attracted to the anode and anions to the cathode. According to Langevin's equation (Ref. 24), mobility of a particle is inversely proportional to its mass. The electrons, due to their extreme lightness, are the major charge carriers. The charge density and the probability of inelastic collisions are greater in the near-electrode regions. The observed voltage drops and temperature profiles (Refs. 25, 26) are proof of inelastic collisions because Ohmic heating is an energy loss manifested by the voltage drop. In the arc column, however, potential drops are smaller, thus causing the carriers to travel with a more uniform and Maxwellian velocity. Despite cooling by the electrodes and the continuous flow of gas, temperatures within the arc column (Refs. 5, 23) are lower than temperatures nearer the electrodes (particularly the cathode, where voltage drops the most).

In GTA welding, cations are generated mainly from the ionization of electrode materials and shielding gas (Refs. 22, 23, 27). With ionic fluxes, anions must also coexist, although their presence within the arc is difficult to confirm. Chemical interactions inside the arc must be hypothesized. For a diatomic chloride, MCl (where M is a metal), the homolytic dissociation to neutral atoms ($MCl \rightarrow M+Cl$) (Ref. 28) is probable, as is the heterolytic dissociation into ions ($MCl \rightarrow M^+ + Cl^-$) (Ref. 28). When the metal is divalent, a reaction with an electron may add an intermediate reaction where an electronegative molecular anion forms ($MCl_2 + e^- \rightarrow MCl^- + Cl$). Regardless of the events, several possibilities support the fact that the element M in a chloride MCl_y ($_y$ being 1 or 2) greatly influences the arc. In a heterolytic dissociation, deionization of the cation, M+, by the capture of electrons is very plausible. If it occurs, reionization of M is made also necessary to maintain the charge carrier population and the current at constant levels. In a homolytic dissocia-

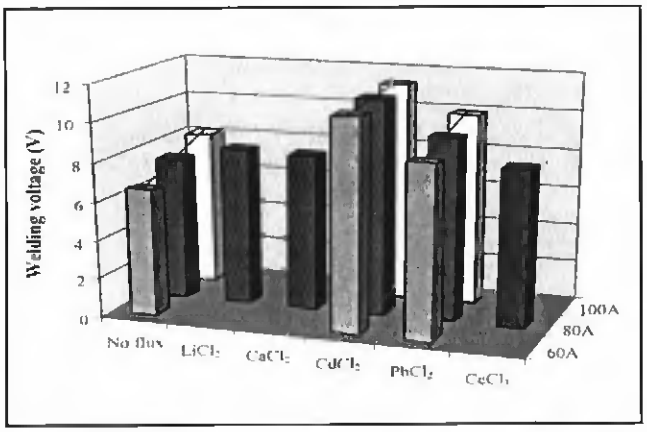

Fig. 3 — Three-dimensional representation showing the effects of different chlorides and currents on welding.

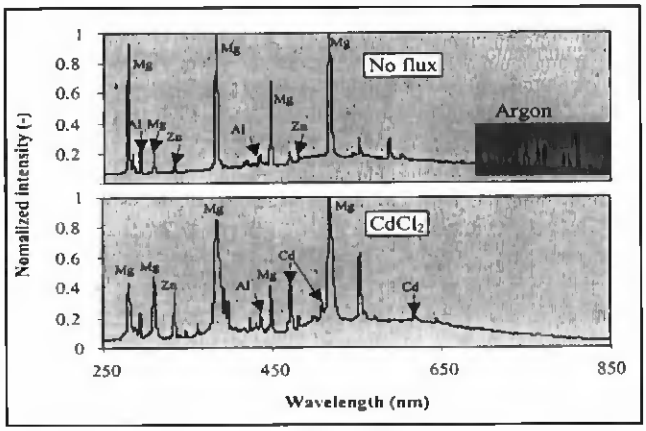

Fig. 4 — Intensity spectra for welds made with and without cadmium chloride at 80 A.

tion, direct ionization of M probably proceeds. The first ionization potential of M is only between 4 and 9 eV, and is considerably lower than that of the noble shielding gases. With elements of low first ionization potential, charge carriers form at lower temperatures and electrical conductivity is normally improved.

However, with ionic compounds, the possible enrichment of the arc with anions (e.g., chlorine ions) seemingly counterbalances the effects of elements that possess a low first ionization potential. Other investigators (Ref. 9) have reported that the welding voltage increased when fluxes were present. This response from the voltage supply to maintain current constant demonstrates arc conductance is reduced by fluxes. With fluxes, current is higher where the density of anions or particles with high ionization potentials is at a minimum. Using this argument, these particles probably do not enter the arc column but segregate to its periphery and force the electrons into a narrower arc column. The contraction of the anode and cathode spots discussed by several authors (Ref.5) substantiates this hypothesis. Saha's equation (Ref. 23), although strictly applicable to equilibrium and ideal gas plasmas, also rationalizes a contraction of the arc and arc column. It predicts that the density of electrons and cations decreases from the central region of the arc toward its periphery where lower temperatures prevail. The hypothetical situation of a flux constricting an arc may thus be analogous to that in forced cooled electrodes and pressurized atmospheres (Ref. 22) where the reduced conductivity of the arc periphery forces the current to pass through a narrower column, causing more collisions and a hotter arc column. Because current flows where conductance is highest, charge carriers first travel straight in the electrode tip extension. As in GTA welding under high current densities, deflection of the arc toward the pool tail may also occur.

Potential Flux-Weld Metal Interactions

The characteristics of fluxes for GTA welding must be speculated because they are unknown. First, the ionic nature of chlorides makes them electrical insulators relative to the electrodes, and in reference to the discussion above, their introduction must affect the arc. Their stability can be predicted from the simplistic concept of electronegativity. As a general rule, the higher the difference of electronegativity between two elements, the greater the bond strength and stability of a compound made of these two elements. Although electronegativity has various definitions, it invariably measures the power of an atom to attract electrons to itself. Pauling electronegativity (Ref. 29) is a well-accepted concept, although it is unitless. The electronegativity as defined by Milliken and Pearson is roughly proportional to the Pauling electronegativity (Ref. 29) and has units of electrovolts (eV). This value has been defined as the sum of the electron affinity and the first ionization potential. Because the electron affinity is less than 10% of the first ionization potential, the first ionization potential is a reasonable approximation of electronegativity. Thus, the difference of electronegativity between two elements can be approximated by their difference of first ionization potentials, and the stability of a chloride MCl_y can be described by the first ionization potential of M only. As discussed above, first ionization potential partially measures the arc current-carrying capability, thus its temperature. Because both stability of chlorides and arc conductance are related to the first ionization potential of M, the element M must be selected so the first ionization potential is widely varied. Chlorides made from alkaline, alkaline earth, rare earth, and other simple-metal elements fulfill this criterion.

After dissociation of MCl_y, the element M must interact with the molten material. Although alloying is probably limited due to dilution (a function of the welding conditions), alloying may still be sufficient to alter weld properties. It is suspected elements with extensive solubility in the magnesium solid phase may be less detrimental. By staying in solution, solute segregation, hard and brittle intermetallic phase formation, and solute effects on solidification must be all reduced. Empirical correlations established that elements with high solid solubility (Ref. 30) in magnesium also have large partitioning coefficients. These elements, with the exception of cadmium, are all eutectic formers, and they change least the freezing range and the solidification cracking susceptibility, as was defined by Borland (Ref. 31). To prevent enhanced corrosion, solute with hydrogen potentials very different from that of magnesium must be avoided. Thus, most transition-metal chlorides are unsuitable, whereas the simple metals (with s and p electrons only) (Refs. 30, 32) satisfy most of the selection criteria. With the exception of cerium chloride, all chlorides of this study included simple-metal elements.

Experimental Procedure

Materials and Welding Procedure

Flux-assisted gas tungsten arc welding was investigated using bead-on-plate experiments on wrought AZ21 magnesium alloy rectangular plates (1.90 wt-% Al; 1.2 wt-% Zn; 0.5 wt-% others; Mg bal.). Specimen dimensions (140 x 70 x 10 mm^3) were chosen to repeatedly guarantee steady-state and three-dimensional heat flow,

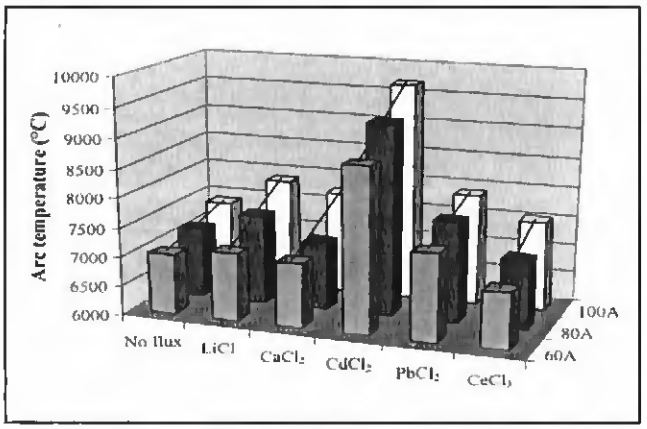

Fig. 5 — Three-dimensional representation showing the effects of different chlorides and currents on arc temperature

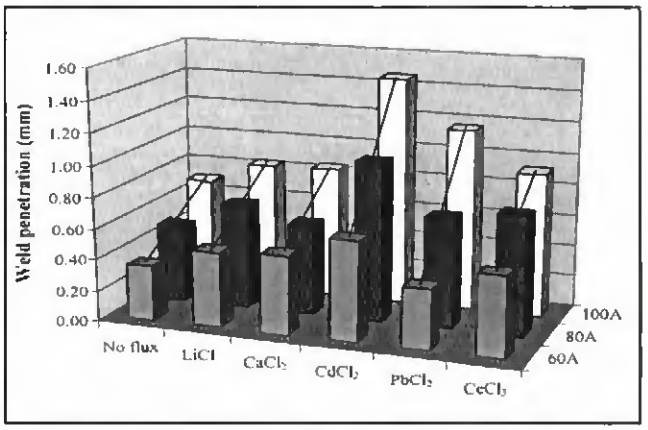

Fig. 6 — Three-dimensional representation showing the effects of different chlorides and currents on weld penetration.

therefore promoting shallow welds with depth-to-width ratios smaller than those encountered in thin specimens where heat flow is two-dimensional (Ref. 33). Before welding, the specimens were ground using up to 600-grit silicon carbide papers. The chlorides were dissolved into distilled water, which was preferred over other liquid media because of enhanced dissolution. Preliminary welds showed this greater dissolution resulted in more uniform flux layers and less erratic welding conditions than with other liquid media. The chlorides were all dissolved up to their respective solubility limit to maximize their effects on welding. Lithium chloride (LiCl), calcium chloride ($CaCl_2$), cadmium chloride ($CdCl_2$), lead chloride ($PbCl_2$), and cerium chloride ($CeCl_3$) were all added to water and used as single-solute ingredients.

Welding experiments were conducted with a 2-mm tungsten cathode delivering a direct current. In all experiments, the torch was set to travel from a bare-metal position to a position surfaced with the selected chloride. After extinction of the arc, the tungsten cathode tip was systematically inspected to ascertain that precedent and subsequent conditions were identical. If changes were observed, the tungsten electrode was replaced by another electrode machined with an identical 60-deg tip. Argon was selected for shielding and supplied at a constant rate of 40 L·min^{-1}, as recommended by handbooks (Ref. 33). The electrode-to-workpiece distance was precisely held at 0.6 mm by means of a standard sheet. Welding currents were between 60 and 100 A, and travel speed was fixed at 12.5 mm·s^{-1}, an abnormally high travel speed selected to reduce the heat input and make weld pool formation more dependent upon the flux. To precisely record the experimental conditions, a current and voltage data acquisition system complemented by emission spectroscopy and digital video recording was used.

After welding, the beads were cross-sectioned, polished, and etched with a slightly acidic solution to reveal the weld interface and the internal microstructure. Fusion zone dimensions and microstructure were analyzed by optical microscopy, microhardness testing, and electron dispersive spectroscopy.

Spectroscopic Survey

Arc temperatures were measured using a single-channel emission spectrometer pointing at the arc central region. The two-line method, which involves measuring radiated intensity at two specific wavelengths, was adopted (Refs. 34, 35). The magnesium lines for excitation of a neutral atom (279.5 nm) and a singly ionized atom (285.2 nm) were preferred over others (such as the argon lines) because they could be separated consistently from the rest of the spectra, regardless of the welding parameters and the fluxes. The temperature, isolated from the Maxwell-Boltzmann statistical term of Equation 1, is expressed as an electron temperature,

$$\frac{I_{Mg0}}{I_{Mg+}} = \frac{n_0 Z_+}{n_+ Z_0} \cdot \frac{A_0 g_0 \nu_0}{A_+ g_+ \nu_+} \cdot exp\left(\frac{E_+ - E_0}{kT}\right) \quad (1)$$

Realistically, the electron temperature differs from temperatures of heavier particles because the conversion of momentum and energy to heat requires time. Although the welding plasma is likely not at equilibrium, thermal equilibrium was assumed, as had been done in other investigations (Refs. 34, 35). In Equation 1, the indices *0* and + apply to neutral and singly ionized atoms, I is the spectrum line intensity, n is the particle density, Z is its internal partition function, A is the transition probability ($A_0 = 2.60 \cdot 10^{-8}$s; $A_+ = 4.95 \cdot 10^{-8}$s) for an electron moving to a lower quantum level (Ref. 29), g is the level of degeneracy of an upper quantum level or statistical weight (Ref. 29), λ is the wavelength associated to this de-excitation (Ref. 29), E is the average energy level ($E_0 = 4.346$ eV; $E_+ = 4.434$ eV) (Ref. 29), and k is the Boltzmann constant. The particle density was determined from Saha's equation (Ref. 23), which assumes the arc behaves as an ideal and homogeneous gas under thermal equilibrium. For the first ionization only, Saha's equation can be expressed as

$$\frac{\alpha^2}{1-\alpha^2} = \left(\frac{2\pi m_e}{h^2}\right)^{\frac{3}{2}} \cdot \frac{(kT)^{\frac{5}{2}}}{p} \cdot \frac{2Z_0}{Z_0} \cdot exp\left(\frac{-E_{Ion}}{kT}\right) \quad (2)$$

where α is the degree of ionization (i.e., the fraction of electrons produced after ionization of a population of neutral atoms), and p is the total pressure, which follows Dalton's law and is approximated as the atmospheric pressure. The partition functions, Z, in Equations 1 and 2 are the sum of all possible energy states of a given particle, here a neutral atom or a cation. The partition function is defined as

$$Z = \sum_i g_i \cdot exp\left(\frac{E}{kT}\right) \quad (3)$$

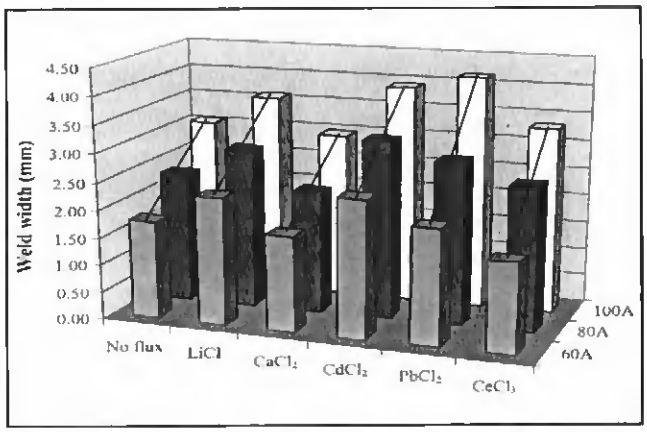

Fig. 7 — Three-dimensional representation showing the effects of different chlorides and currents on weld width.

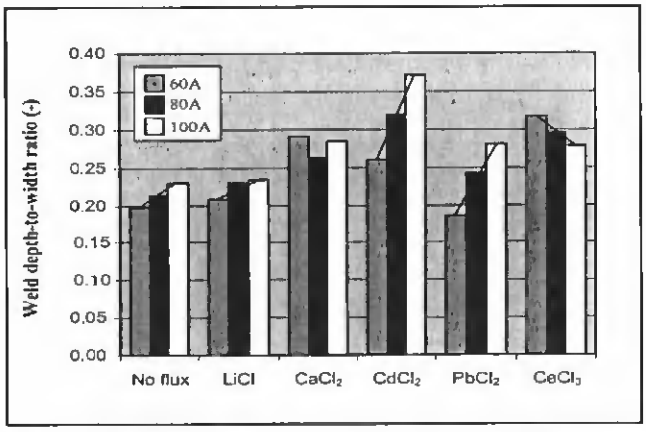

Fig. 8 — The effects of chlorides and welding current on weld depth-to-width ratio.

The temperatures derived from emission spectroscopy often have been questioned. The method applied here to determine the arc temperature was clearly imperfect but sufficient for comparing the effects of chloride fluxes. Due to spectral line preferences, statistical weights were within a 25% error. Although such uncertainties affect temperature determination, Saha's remained most influential. The concepts of equilibrium and ideal gas behavior for a welding arc (Ref. 23) are simplistic, mainly because charged particles interact. However, without better means of approximation for the ionization degree, Saha's equation remains the best approximation. Also, since the same method was applied in all calculations of the temperature, similar errors were made with each chloride. Note that emission spectroscopy was not intended to determine arc temperature distribution, where a more advanced apparatus would have been required, but was used only to estimate a mean arc temperature, as one would evaluate the arc resistance rather than a spatial distribution of its resistivity.

Results and Discussion

The results of experiments related to the electric arc, the morphology, and the microstructures of the weld fusion zone are consecutively discussed to clarify the role of the chloride fluxes. Because chloride properties depend upon temperature, their effects must differ at elevated temperature (when they are dissociated) and at low temperature. Hence, the possibility that their contribution changes with the process parameters was also important to addressed.

Arc Profiles

The role of chloride fluxes during FA-GTA welding was first investigated using video recording. The images shown in Fig. 1 provide clear experimental verification of the influence of chlorides on the electric arc. Figure 1 illustrates the effect of cadmium chloride by comparing front view (left image) and side view (right image) profiles left by the arc in the CCD camera during chloride-assisted GTA welding (bottom images) and normal GTA welding (top images). The border of the brightest region on the images is a contour of constant intensity that provides a magnified view of the electric arc. Regardless of the view angle, Fig. 1 shows the brightest region was roughly 100% broader when cadmium chloride was present. Additional images taken when the other chlorides were applied have confirmed the enlargement of the brightest region, although enlargement was less. Based upon these results, cadmium chloride was given more attention during the rest of this study.

The changes in arc profile with the chloride fluxes, as shown in Fig. 1, are intriguing. Although a thorough experimental verification is lacking, the arc profiles resemble a high-pressure jet that impacts a flat solid surface and is dispersed sidewise. The front views suggest the metal vapors from the anode region were spread sidewise when chlorides were present. The side views reveal the electric arc was deflected toward the weld pool rear in the presence of cadmium chloride. This arc deflection indicates the preset current was not restricted to the area straight beneath the cathode tip. With fluxes, it is clear the charge carriers were redistributed and the enlargement of the brightest region, although not quantified, must relate to visible emission intensity and, thus, to the arc temperatures and welding voltage.

Welding Voltage

Figure 2 shows voltage values during the welding of a specimen that was half coated with a thin layer of cadmium chloride. It can be seen the voltage stepped up rapidly when the arc encountered the flux. Because current is self-adjusted to its selected value, the increase in voltage corresponds to a comparable increase in heat input, both quantities being approximately proportional. Figure 3 is a three-dimensional graphical representation that summarizes the influence of both the chlorides and the current on the voltage. It is clear that not only cadmium chloride but also all chlorides increased the voltage. The increases caused by the chlorides can be weak or strong, depending upon their chemical composition and the current.

Increases of voltage first suggest weld pool formation only occurred after the flux layer had been broken up and possibly removed from the arc column. This process of displacing the flux, either by vaporization or fluid flow, is energy consuming. The increases of voltage, which can be interpreted as a strengthening of the electrical fields, indicate greater energies. Based upon Fig. 3, different chlorides therefore require different energies before the selected current (i.e., 60, 80, 100 A) reaches the pool.

Comparisons of various chlorides at a fixed current (e.g., 80 A) reveal cadmium chloride raised voltage the most by approximately 3.5 V beyond the voltage established without fluxes. The results with cadmium chloride were not surprising judging from the video observations. Cadmium chloride was followed by lead chloride, which augmented the voltage about 2 V. The other chlorides also increased voltage, but moderately (~0.5 V), which made all of them rather indistinguishable. The fact cadmium and lead are also the elements with the highest first ionization potentials must not be coincidental. As discussed previously, elements of high first ionization potential necessitate

Fig. 9 — Optical micrographs of GTA (left) and FA-GTA (right) weld cross sections (cadmium chloride flux).

greater temperatures to release a first electron. Because electrical conductivity depends upon electron density, conductivity is lower with elements of high first ionization potential. The ohmic impedance of the arc, defined by the ratio of the voltage to the current, is greater with cadmium chloride (11 V/80 A) and lead chloride (9.3 V/80 A). The heat dissipated by the joule effect, indirectly given by the heat input, and the average arc temperature must also be greater with those two chlorides.

As expected from Ohm's law, Fig. 3 also shows that increases in voltage correspond to increases in current. However, due to experimental difficulties, correlation between voltage change and current change for the various chlorides were not satisfactorily completed. Figure 3 shows that several data are missing to determine the voltage-current line slope, a quantity that would have allowed a precise evaluation of the ohmic impedance caused by each chloride.

Arc Emission Spectra

Like Fig. 2, where voltages with and without cadmium chloride are compared, Fig. 4 shows the corresponding normalized emission spectra. In the absence of fluxes, the most intense peaks were those of magnesium, aluminum, and argon. With cadmium chloride, the neutral argon peaks were observed to disappear unless current was increased. The observation that greater currents were needed to resolve the argon lines has at least two explanations. Electron excitation of the neutral and ionized argon atoms might have been small, thus implying arc temperatures were lower with cadmium chloride. However, this possibility is questionable in view of other results, and a second possibility must be considered. Because measurements were conducted near the weld pool, fumes containing flux ingredients might have interfered with the argon flow reaching the weld surface. The choice of peaks of either magnesium or aluminum was unavoidable. Because the magnesium peak at 518.0 nm was always highest, it was selected. The fact that several magnesium lines for both the neutral atom (385.0, 518.3, 552.8 nm) and the first cation (279.5, 448.1 nm) were always identifiable and highest suggests magnesium was the dominant emitting specie, although radiations of other elements contained in the fluxes were also detected.

Figure 5 summarizes the temperatures derived from the emission spectra corresponding to the voltages of Fig. 3. When compared to other studies (Refs. 34, 35), the temperatures shown in Fig. 5 are low, as was suggested from the argon emission that was frequently within the background noise. Compared to parameters used in investigations with different materials (Refs. 34, 35), the electrode-to-work distance (0.6 mm) and currents (less than 100 A) in this study were significantly smaller. As for the voltage, the arc temperature increased with the current. The highest temperatures were with cadmium chloride. Despite uncertainties, the arc temperatures associated with lead chloride were the second highest. Cadmium and lead are the elements with the first and second highest ionization potentials among all the elements, M, for the selected chlorides MCl_y. The observation that arc temperature increased with the first ionization potential of M is not a discovery, but the fact that the metallic component, M, of the chloride MCl_y can simply explain the chloride contribution is a new conclusion. Eastern European investigators (Ref. 5) established a linear relationship between first ionization potential and temperature, wherein temperature equaled 800 times the first ionization potential of the element. When this simple relationship is applied, the temperatures reported in this study are substantiated. Although first ionization potential is important, it is undeniably not the only key variable. The weld morphology data can help in identifying elements having a low first ionization potential, but also producing deep and narrow welds.

Weld Morphology

Figures 6–8 are graphical representations depicting the variations of weld fusion zone dimensions with both various chlorides and welding currents. All chlorides enhance weld penetration, weld width, and weld depth-to-width ratio. Increases in weld dimensions with chlorides were either weak or strong, depending upon chemical composition and current.

Figure 6 reveals cadmium chloride, again followed by lead chloride, then cerium chloride, and lithium chloride, maximized weld penetration. In comparison, calcium chloride had a minor effect. Figure 7, which focuses on the weld width, shows that cadmium chloride and possibly lead chloride were best, followed by lithium chloride and cerium chloride. Calcium chloride was not observed to widen the fusion zone. On the contrary, it possibly promoted narrower weld beads. As a first approximation, the rankings of the chlorides, as measured by effects on voltage (Fig. 3), arc temperature (Fig. 5), weld penetration (Fig. 6), and weld width (Fig. 7), were similar. Cadmium (8.993 eV) and lead (7.416 eV) possessed the highest first ionization potentials, and always produced the most distinct results.

As for other characteristics, the effect of current alone was readily predictable. Figure 3 showed current and voltages were related as in Ohm's law. Consequently, the

heat dissipated by the arc and its temperature, as confirmed in Fig. 5, increased with the current. As depicted in Figs. 6 and 7, both penetration and width also increased monotonically with the current, regardless of the chloride present. Figures 6 and 7 not only demonstrated that cadmium chloride and lead chloride produced greater penetration and width but also suggested weld penetration increased most significantly with these two chlorides. Just as the slope of the tension-current line approximates an impedance, the slope of a dimension-current line quantifies the augmentation in weld dimensions. For cadmium chloride and lead chloride, Figs. 6 and 7 show straight lines with these two chlorides were steepest, having slopes near 0.02 mm A^{-1} for the penetration and 0.04 mm·A^{-1} for the width. In agreement with previous data, the remaining chlorides (i.e., cerium chloride, lithium chloride, and calcium chloride) exhibited fusion zone dimensions that varied little with the current. While correlations with voltage or temperature were partially expected, no obvious correlation between slopes is apparent. The fact that cadmium chloride and lead chloride showed similar variations is difficult to rationalize from the first ionization potential alone.

Unlike the increases in dimensions with current, depth-to-width ratios were occasionally unexpected, thus implying first ionization potential of M provides an incomplete explanation. Figure 8 shows cadmium chloride produced the greatest depth-to-width ratio. Also, cadmium chloride and lead chloride revealed the same relative potency encountered for penetration, because the rates at which the depth-to-width ratio changes with the current were comparable for both chlorides, despite the fact cadmium chloride produced appreciably greater values. This observation is unexplained and may require consideration of other contributions. The results with calcium chloride were different from those with cerium chloride, where depth-to-width ratios decreased with the current. If it is hypothesized the depth-to-width ratio measured the potency of a chloride to alter the heat flux so deep and narrow welds may be promoted, then cadmium chloride was best. On the other hand, cerium chloride lost this effectiveness when current was increased. The first ionization potential of cerium is clearly insufficient to explain these results. Although it is now clear the first ionization potential controls arc voltage and arc temperatures, it remains unexplained how those two effects could be related to arc constriction. A strong possibility exists that arc constriction indeed increases the arc voltage and the temperature. A good explanation for why calcium chloride created a greater depth-to-width ratio than lead chloride is missing. Likewise, a reason for why similar depth-to-width ratios were obtained by adding either lead chloride or lithium chloride is not available.

Weld Microstructure

In previous discussion, the alloying with magnesium of the element M included in the chloride MCl_y was considered. These various elements were specifically selected to stay in solid solution so as to minimize changes in both microstructure and properties. Microhardness indentations did not reveal any appreciable differences within the fusion zones produced using chloride additions; Vickers microhardness averaged 48 with or without chloride flux. Chemical compositions measured by electron dispersive spectroscopy showed metallic elements of the flux were present in the fusion zone, but within the uncertainty of measurements (<0.5 wt-%). Although partially inconclusive, the results confirmed that alloying from the flux probably did not drastically affect the solute partitioning during solidification.

When micrographs of fusion zones created both with and without chlorides were compared (Fig. 9), differences could be seen. In the GTA welds (Fig. 9B), the solidification microstructure was columnar throughout the entire fusion zone. With identical process parameters, the fusion zone created using the cadmium chloride flux (Fig. 9B) was significantly more dendritic. Although columnar dendrites were still observed at the fusion boundary (a preexisting solid-liquid interface has no nucleation barrier and growth often is epitaxial), the remainder of the fusion zone exhibited fine dendrites. A transition between the columnar-to-dendritic regions was markedly visible in the FA-GTA welds, as shown in Fig. 9B.

In arc welding, constitutional undercooling, determined by the ratio of the thermal gradient and growth rate (Ref. 36), controls the solidification microstructure. Since travel speed and solidification rates are proportional (Ref. 36), solidification rates were unchanged. Differences in microstructure between welds with and without chlorides must therefore arise from the thermal gradient. With cadmium chloride, the arc temperature was significantly higher and the fusion zone microstructure substantiates an increase in constitutional undercooling; i.e., an increase in the thermal gradient. To increase the thermal gradient, heat extraction in the presence of chloride fluxes had to be faster. A more intense weld pool circulation would have certainly assisted the thermal conduction and would have promoted greater thermal gradients.

Conclusions

The influences of metal chloride fluxes on the electric arc and weld fusion zone have been discussed. Although welding with chloride fluxes is complicated, a straightforward relationship between weld morphology and first ionization potential has been proposed. While further investigation is required to thoroughly understand the FA-GTA welding of magnesium alloys, the following conclusions were reached:

- All selected chlorides affected cross-sectional fusion zone dimensions. More specifically, chlorides increased the weld penetration and the weld bead depth-to-width ratio.
- The extent of weld bead morphological changes depended upon the specific chloride and process parameters. A flux that is insensitive to the process parameters must, therefore, be made of several ingredients.
- Increases in weld penetration were accompanied by increases in voltage and, therefore, heat input. As a first approximation, arc temperature, voltage, and first ionization potential of the element M in the chloride MCl_y correlated.
- Of all selected chlorides, cadmium chloride was the most effective in altering weld bead morphology. Weld penetration was increased by more than one hundred percent. The effectiveness of lead chloride followed that of cadmium chloride. Cadmium and lead have the two highest first ionization potentials of all the elements selected for this study.
- Captured images of the arc region during welding both with and without chlorides demonstrated noticeable differences. The heat flux from the arc appeared more concentrated toward the center of the pool when chlorides were present.
- The actual mechanisms for the changes in weld bead morphology remain uncertain. Elements possessing high first ionization potential produced hotter arcs, but arc constriction could not be verified. Likewise, any contribution from a surface-energy driven flow proved equally difficult to establish.

Acknowledgments

M. Marya would especially like to thank S. Patay and M. Matsushita for their assistance in the use of the emission spectrometer. The assistance of M. Shaba from Ecole Centrale Nantes in the use of the digital video camera is also greatly appreciated. The authors are very grateful for an American Welding Society Fellow-

ship for M. Marya and for funding provided by Visteon Automotive Systems (Dearborn, Mich.).

References

1. Gurevich, S. M., Zamkov, V. N., and Kushmienko, N. A., 1965. Increase in the efficiency of penetration of titanium alloys in argon-arc welding. *Avtomaticheskaya Svarka* 9: 1–4.

2. Gurevich, S. M., and Zamkov, V. N. 1973. Metallurgical and technological features of titanium alloy welding when using fluxes. *Titanium Science and Technology*. New York-London: Plenum Press. pp. 541–551.

3. Simonik, A. G. 1974. Effect of halides on the penetration in argon and welding titanium alloys. *Svar. Proiz* 3:52–53.

4. Paskell, T., Lundin, C., and Castner, H. 1997. GTAW flux increases weld joint penetration. *Welding Journal* 76(4): 57–62.

5. Paton, B. E., Zamkov, V. N., Prilutsky, V. P., and Poritsky, P. V. 2000. Contraction of the welding arc caused by the flux in tungsten-electrode argon-arc-welding. *Paton Welding Journal* 1: 5–11.

6. Perry, N., Marya, S., and Soutif, E. 1998. Study and development of flux enhanced GTA penetrations in a commercial grade titanium. *Proceedings of 5th International Conference on Trends in Welding Research* (ASM/AWS), pp. 520–525. Pine Mountain, Ga.

7. Lucas, W., and Howse, D. 1996. Activating flux — increasing the performance and productivity of the TIG and plasma processes. *Welding and Metal Fabrication* 1: 11–17.

8. Sire, S., and Marya, S. K. New perspective in GTA welding of carbon steels by the use of silica. Accepted for publication in *International Journal of Forming Processes.*

9. Middel, W., and Den Ouden, G. 1998. The effect of additives on arc characteristics in GTA welding. *Proceedings of 5th International Conference on Trends in Welding Research* (ASM/AWS), pp. 394–399. Pine Mountain, Ga.

10. Tanaka, M., Shimizu, T., Terasaki, H., Ushio, M., Koshi-ishi, F., and Yang, C. L. 2000. Effects of activating flux on arc phenomena in gas tungsten arc welding. *Science and Technology of Welding and Joining* 5(6): 397–402.

11. Heiple, C. R., and Roper, J. R. 1982. Mechanism for minor element effects on GTA fusion zone geometry. *Welding Journal* 61(4): 97-s to 102-s.

12. Heiple, C. R., Roper, J. R., Stagner, R. T., and Aden, R. J. 1983. Surface active elements effects on the shape of GTA, laser and electron beam welds. *Welding Journal* 62(3): 72-s to 77-s.

13. Mills, K. C., and Keene, B. J. 1990. Factors affecting variable penetration. *International Materials Review* 35(4): 185–216.

14. Pollard, B. 1988. The effects of minor elements on the welding characteristics of stainless steels. *Welding Journal* 67(9): 202-s to 213-s.

15. Pierce, S. W., Burgardt, P., and Olson, D. L. 1999. Thermocapillarity and arc plasma in stainless steel welding. *Welding Journal* 78(2): 45-s to 52-s.

16. Kittel, C. 1996. *Introduction to Solid State Physics*, Seventh ed. John Wiley and Sons, Inc.

17. Neff, D. V. 1988. Nonferrous molten metal processes. *ASM Handbook — Casting*. Vol. 15, pp. 445-496. Materials Park, Ohio: ASM International.

18. Hunter, G., Kenney, G. B., Ring, M., Russel, B. A., and Eagar, T. W. 1978. Submerged arc welding of titanium. Report AD-A085. Cambridge, Mass.

19. Marya, S., and Lemaitre, F. 1980. On the elaboration of a new submerged arc welding flux for titanium. *J. Less Common Met.* 69(1): 195–202.

20. Practical Briefs. 1972. Materials — alloy types and fluxes. *Welding Journal* 51(8): 571–577.

21. Jarvis, B. L., Ahmed, N. U. 1998. The behavior of oxide films during gas tungsten arc welding of aluminum alloys. *Proceedings of 5th International Conference on Trends in Welding Research* (ASM/AWS), pp. 410–414. Pine Mountain, Ga.

22. Jackson, C. E. The science of arc welding. Internal document of the Union Carbide Corporation, No. 52–501, also published in the *Welding Journal* with the following references: 1960, 39(4): 129-s to 146-s, 39(5): 177-s to 190-s, 39(6): 225-s to 230-s.

23. Lancaster, J. F. 1984. *The Physics of Welding*. Pergamon Press.

24. Chen, F. F. 1984. *Introduction to Plasma Physics and Controlled Fusion*, Second ed. Plenum Press.

25. Key, J. F., Chan, J. W., and McIlwain, M. E. 1983. Process variable influence on arc temperature distribution. *Welding Journal* 62(7): 179-s to 184-s.

26. Petrie, T. W., and Pfender, E. 1970. The influence of the cathode tip on temperature and velocity fields in gas-tungsten arc. *Welding Journal* 49(12): 588-s to 596-s.

27. Dunn, G. J., Allemand, C. D., and Eagar, T. W. 1986. Metal vapor in gas tungsten arcs — part I. Spectroscopy and monochromatic photography. *Metallurgical Transaction A*. 17A(10): 1851–1863.

28. *Halogen Chemistry*. 1967. Ed. V. Gutman. Academic Press.

29. *CRC Handbook of Physics and Chemistry*. Boca Raton, Fla.: CRC Press.

30. Marya, M., Patay, S., Marya, S. K., and Edwards, G. R. 2001. Fundamental aspects in the joining of magnesium alloys by the GTAW and LBW processes. To be published in the *Proceedings of IWC 2000*, New Delhi, India.

31. Borland, J. C. 1961. *British Welding Journal* 8: 526–540.

32. Hume-Rothery. 1967. *Acta Metallurgica* 14(1): 17–20.

33. *ASM Handbook — Welding, Brazing, and Soldering*, Vol. 6. 1993. Materials Park, Ohio: ASM International.

34. Glickstein, S. S. 1976. Temperature measurements in a free burning arc. *Welding Journal* 55(8): 222-s to 299-s.

35. Key, J. F., Chan, J. W., and McIlwain, M. E. 1987. Process variable influence on arc temperature distribution. *Welding Journal* 62(7): 179-s to 184-s.

36. David, S. A., and Vitek, J. M. 1989. Correlation between solidification parameters and weld microstructures. *International Materials Review* 34(5): 213–245.